Photochemistry and Photobiology, 2011, 87: 1204–1213

Invited Review

Photosensitization Reactions *In Vitro* and *In Vivo*

Bonnie I. Kruft and Alexander Greer*

Department of Chemistry, Graduate Center & The City University of New York (CUNY), Brooklyn College, Brooklyn, NY

Received 25 June 2011, accepted 18 August 2011, DOI: 10.1111/j.1751-1097.2011.00993.x

ABSTRACT

This review of *Photochemistry and Photobiology* summarizes articles published in 2010, and highlights progress in the area of photosensitization. The synthesis of conjugated photosensitizers is an area of interest where increasing water solubility has been a goal. Targeting infrared sensitizer absorption has been another goal, and relates to the practical need of deep tissue absorption of light. Photodynamic techniques for inactivating microbes and destroying tumors have been particularly successful. Biologically, singlet oxygen [$^1O_2(^1\Delta_g)$] is an integral species in many of these reactions, although photosensitized oxidations tuned to electron and hydrogen transfer (Type I) give rise to other reactive species, such as superoxide and hydrogen peroxide. How photoprotection against yellowing, oxygenation and degradation occurs was also an area of topical interest.

This review is only a sampling of papers published in 2010 in *Photochemistry and Photobiology* covering the area of photosensitization, wishing to highlight readers on some of the advancements that were made. The review has four sections: photosensitizer design; supports for or encapsulation of photosensitizers; photooxidation and photoprotective reactions and photodynamic action. A summary table shows photophysical data of the sensitizers and trapping agents (Table 1).

PHOTOSENSITIZER DESIGN

The synthesis of conjugated photosensitizers represents an area that is of interest to photochemists where increasing water solubility has been a goal. As would be expected, the water solubility of C_{60}-D-glucose (**1**) and C_{60}-maltohexaose (**2**) photosensitizers was enhanced compared to C_{60} itself (Scheme 1) (1). Upon irradiation with UVA light, the cytotoxicity of **1** and **2** against several cancer cell lines was attributed to singlet oxygen. A Rose Bengal-linker-penicillanic acid (**3**) and a Rose Bengal-linker-kanamycin conjugate (**4**) were found to be bactericidal agents under white light irradiation; they led to the eradication of *Staphylococcus aureus* and *Escherichia coli*, respectively, under conditions where Rose Bengal and kanamycin individually were ineffective (2). Cyclometalated complexes included a [Pt(Thpy)(HThpy)pyridine]$^+$ (**5**) and a thienyl/pyridyl Pt(II) butoxycalix[4]arene (**6**) (3), where O_2 quenched the metal-to-ligand charge transfer excited states producing $^1O_2$ in high yields. In CD_3CN, the $^1O_2$ quantum yield (Φ_Δ) of **5** approached or exceeded 0.95 (Table 1). Sensitizer **5** was examined and was shown to be photocytotoxic to HeLa cells.

Targeting redshifted sensitizer absorption has been a goal, and relates to practical needs such as deep tissue absorption of light. Hypericin hydroquinone (**7**) was redshifted compared to hypericin itself, and exhibited photocytotoxicity on DU145 human prostate carcinoma cells (Scheme 2) (4). One problem was the stability; there was the tendency of the hydroxy groups of **7** to revert to the keto form of hypericin. Somewhat structurally similar to hypericins are the hypocrellins. Sodium hypocrellin B-aminododecanoate (**8**) and sodium hypocrellin B-dimercaptoundecanoate (**9**) were synthesized (5), and had surfactant-like properties, arguably more amphiphilically compatible to blood plasma for cellular uptake. Sensitizer **9** was active against human breast carcinoma MCF-7 cells, where singlet oxygen was formed; however, under anoxic conditions species such as the semiquinone radical anion were formed.

Water-soluble Zn-azaphthalocyanine (**10**) and Zn-azanaphthalocyanine (**11**) were synthesized, each carrying eight quaternary ammonium groups (Scheme 3) (6). Sensitizers **10** and **11** absorbed in the red, had high singlet oxygen quantum yields (Φ_Δ), and localized within the lysosomes of Hep2 cells. Other phthalocyanines studied include a series of chiral *bis*-acetal porphyrazine derivatives, synthesized for absorption and emission in the red (7). The phthalocyanines took the form M[pz($A_{4-n}B_n$)], in which the pyrrole ring contained A = (2R,3R) 2,3-dimethyl-2,3-dimethoxy-1,4-diox-2-ene, B = β,β'-diisopropoxybenzo, M is Zn ion or two hydrogen atoms and n = 0, 1, 2 (*-cis/-trans*) or 3. Of the series, porphyrazine H_2[pz(*trans*-A_2B_2)] (**12**) performed the best, with a dual function of high phototoxicity and strong fluorescence upon uptake by cells.

Zn- and Pd-bacteriopheophorbide (**13** and **14**), and the water-soluble Pd-bacteriopheophorbide (**15**) were studied with near-IR radiation in human blood plasma (Scheme 4) (8). The range of photodynamic damage was suggested to be extended by the formation of peroxides *via* pigment-loaded LDL and HDL. Pd-bacteriopheophorbide **14** had greater stability than

*Corresponding authors email: agreer@brooklyn.cuny.edu (Alexander Greer)

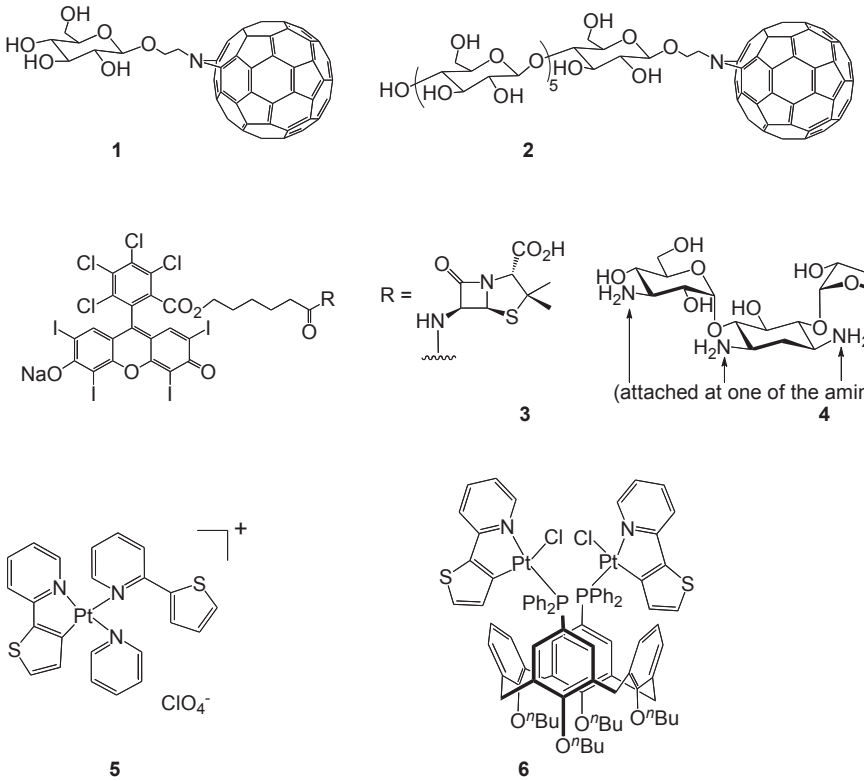

Scheme 1.

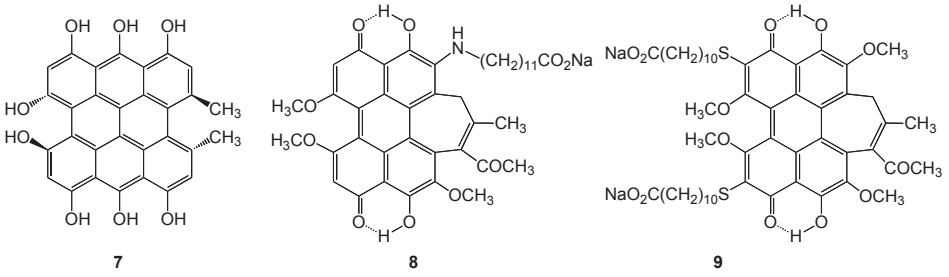

Scheme 2.

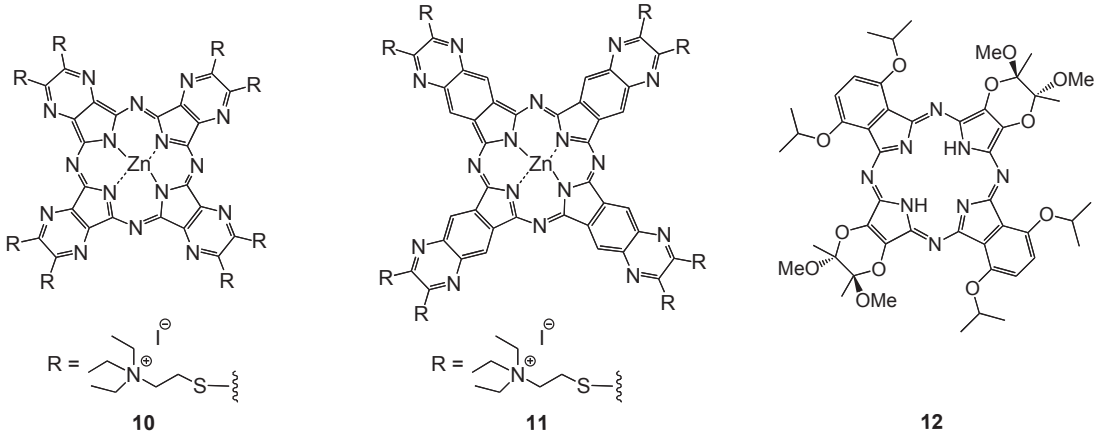

Scheme 3.

13 and **15**, and also produced more reactive oxygen species (ROS) thereby generating hydroperoxides. Another porphyrin system was studied, namely 5,10,15,20-tetra-(phenoxy-3-carbonyl-1-aminonaphthyl)-porphyrin (**16**), which was synthesized by a naphthylisocyanate condensation reaction (9). The absorption of the 4th Q-band extended out to *ca* 670 nm, while

Table 1. Photophysical data of the sensitizers and trapping agents.

Compound	λ_{max} (nm)	λ_{em} (nm)	Luminescence lifetime (τ, μs)	Fluorescence quantum yield (Φ_F)	Singlet oxygen quantum yield (Φ_Δ)	Total (k_T) and chemical (k_r) quenching rate constants of $^1O_2$ (M^{-1} s^{-1})	Photodegradation quantum yield	Ref.	Comments
3	565 (CH_3OH)	–	–	–	–	–	–	2	
4	530 (CH_3OH)	–	–	–	–	–	–		
5	554 (CH_3CN)	–	24 (N_2) 0.33 (air)	0.38 (CH_3CN)	0.95 ± 0.05 (CD_3CN) 0.27 ± 0.03 (CD_2Cl_2)	k_T = 5.54 ± 0.03 × 10^7	–	3	Methylene blue (MB) Φ_F = 0.57 (CD_3CN) and C_{60} Φ_F = 1.00 (CD_2Cl_2) was used as reference
6	559 (CH_3CN)	–	1.38 (N_2) <0.1 (air)	0.021 (CH_3CN)	0.42 ± 0.03 (CD_3CN) 0.15 ± 0.03 (CD_2Cl_2)	k_T = 0.91 ± 0.11 × 10^7	–		
7	525 (DMSO)	–	–	–	–	–	–	4	Sizable absorption peaks were located at 645 and 685 nm
8	460, 580 near equivalent ($CHCl_3$)	–	–	–	1.0 (C_6H_6)	–	–	5	Hypocrellin B Φ_Δ = 0.76 was used as reference
9	526 ($CHCl_3$)	–	–	–	0.93 (C_6H_6)	–	–		
10	656 (DMF)	661 (DMF) λ_{ex} = 375 nm	–	0.058 (DMF)	0.196 (DMF) 0.726 (DMF/HCl)	–	–	6	ZnPc Φ_F = 0.20 (pyridine) and Φ_Δ = 0.56 (DMF) was used as reference. [HCl] = 5 × 10^{-4} M
11	748 (DMF)	751 (DMF) λ_{ex} = 375 nm	–	0.027 (DMF)	0.754 (DMF) 0.677 (DMF/HCl)	–	–		
12	629 (CH_2Cl_2)	462 (CH_2Cl_2) λ_{ex} = 446 nm 727 (CH_2Cl_2) λ_{ex} = 702 nm	–	0.09 (CH_2Cl_2)	0.074 ± 0.001 (CH_3OH) 1.00 ± 0.025 (PC liposome)	–	–	7	The phosphatidyl choline (PC) liposome binding constant K_b was 26.8 ± 1.3 $(mg/mL)^{-1}$
13	*ca* 660 Q-band region	–	–	–	–	–	–	8	Absorption spectra in LDL, HDL or DMSO solutions
14	*ca* 685 Q-band region	–	–	–	–	–	–		
16	420 Soret 514 Q_y(1–0) (toluene)	652 (toluene) Q(0–0) 718 (toluene) Q(0–1)	–	0.086 (toluene)	0.60 (toluene)	–	4.65 × 10^{-4} (azobenzene)	9	Triplet lifetimes were 44.9 ± 1.0 μs (N_2) and 320.6 ± 12.8 ns (O_2) Photodegredation quantum yield was measured with 5,10,15-20-tetraphenylporphyrin Φ_F = 0.11 (toluene) as a reference

Table 1. Continued.

Compound	λ_{max} (nm)	λ_{em} (nm)	Luminescence lifetime (τ, μs)	Fluorescence quantum yield (Φ_F)	Singlet oxygen quantum yield (Φ_Δ)	Total (k_T) and chemical k_r) quenching rate constants of $^1O_2$ (M^{-1} s^{-1})	Photodegradation quantum yield	Ref.	Comments
17	678 Q(0,0) (toluene)	–	–	0.33 ± 0.04 (toluene) 0.20 ± 0.04 (Cremophor RH 40) 0.34 ± 0.07 (Lutrol F 127–Cremophor RH 40)	0.69 ± 0.13 (toluene) 0.40 ± 0.10 (Cremophor RH 40) 0.60 ± 0.10 (Lutrol F 127–Cremophor RH 40)	–	–	14	Hydroxyaluminum tricarboxymonoamidepht-halo-cyanine (AlTcPc) Φ_F = 0.42 (DMSO) was used as reference in toluene. Cresyl violet perchlorate (CV) Φ_F = 0.60 (cellulose) was used as reference in the gel samples. MB Φ_Δ = 0.56 (DMF) was used as reference. The hydrophilic gel was Cremophor® RH40 25% wt/wt. The lipophilic gel was Lutrol® F127 15%, Cremophor® RH40 10% and polypropylene glycol 15%
18	676 Q(0,0) (toluene)	–	–	0.31 ± 0.03 (toluene) 0.21 ± 0.04 (Cremophor RH 40) 0.35 ± 0.06 (Lutrol F 127–Cremophor RH 40)	0.66 ± 0.13 (toluene) 0.60 ± 0.10 (Cremophor RH 40) 0.60 ± 0.10 (Lutrol F 127–Cremophor RH 40)	–	–		
19	673 Q(0,0) (THF)	–	–	0.28 ± 0.06 (THF) 0.02 ± 0.06 (Cremophor RH 40) 0.06 ± 0.03 (Lutrol F 127–Cremophor RH 40)	0.70 ± 0.10 (THF) 0.13 ± 0.06 (Cremophor RH 40) 0.20 ± 0.05 (Lutrol F 127–Cremophor RH 40)	–	–		
20	704 Q(0,0) (THF)	–	–	0.26 ± 0.03 (THF) 0.02 ± 0.05 (Cremophor RH 40) 0.04 ± 0.03 (Lutrol F 127–Cremophor RH 40)	0.69 ± 0.05 (THF) 0.14 ± 0.05 (Cremophor RH 40) 0.26 ± 0.05 (Lutrol F 127–Cremophor RH 40)	–	–		
21	340 (H_2O)	–	–	–	–	–	–	15	
22	311 (H_2O)	390 (H_2O) λ_{ex} = 310 nm	–	–	–	–	–		
23	–	350 (H_2O) λ_{ex} = 338 nm 350 (H_2O, 1 $(mg/mL)^{-1}$ DOPC) λ_{ex} = 338 nm	–	–	–	$k_T = 0.94 \pm 0.09 \times 10^8$ (D_2O/H_2O) $k_r = 0.23 \pm 0.02 \times 10^8$ (D_2O/H_2O) $k_T = 1.7 \pm 0.2 \times 10^8$ [1 $(mg/mL)^{-1}$ DOPC] $k_r = 0.2 \pm 0.2 \times 10^8$ [1 $(mg/mL)^{-1}$ DOPC]	–	16	D_2O/H_2O mixtures were used. 1,2-di-oleoyl-glycero-3-phosphatidylcholine (DOPC) large unilamellar vesicles. The rate constants were "apparent" k_T and k_r quenching values
24	–	355 (H_2O) λ_{ex} = 338 nm 338 (H_2O, 1 $(mg/mL)^-$ DOPC) λ_{ex} = 338 nm	–	–	–	$k_T = 1.8 \pm 0.2 \times 10^8$ (D_2O/H_2O) $k_r = 0.22 \pm 0.02 \times 10^8$ (D_2O/H_2O) $k_T = 2.6 \pm 0.2 \times 10^8$ [1 $(mg/mL)^{-1}$ DOPC] $k_r = 0.56 \pm 0.05 \times 10^8$ [1 $(mg/mL)^{-1}$ DOPC]	–		
27	232 (H_2O)	–	–	–	–	–	0.014 (1.27 mM O_2) 0.018 (0.27 mM O_2) 0.027 (< 50 μM O_2)	18	Photodegradation quantum yields were measured at λ_{ex} = 254 nm in H_2O (pH = 5.4)

Table 1. Continued.

Compound	λ_{max} (nm)	λ_{em} (nm)	Luminescence lifetime (τ, μs)	Fluorescence quantum yield (Φ_F)	Singlet oxygen quantum yield (Φ_Δ)	Total (k_T) and chemical (k_r) quenching rate constants of $^1O_2$ (M^{-1} s^{-1})	Photodegradation quantum yield	Ref.	Comments
28	–	–	–	–	–	$k_T = 0.031 \times 10^8$ (CH_3OH) $k_r = 0.011 \times 10^8$ (CH_3OH)	–	20	CH_3OH solutions contained riboflavin and 10 mM KOH
29	–	–	–	–	–	$k_T = 0.39 \times 10^8$ (CH_3OH) $k_r = 0.3 \times 10^8$ (CH_3OH)	–		
30	–	–	–	–	–	$k_T = 0.009 \times 10^8$ (CH_3OH) $k_r = 0.001 \times 10^8$ (CH_3OH)	–		
31	*ca* 390 (CH_3CN)	–	–	–	–	$k_T = 4.8 \pm 0.1 \times 10^8$ (D_2O buffer, pD *ca* 7.2)	–	25	Alkaline D_2O experiment assumed **33** to be fully ionized
32	*ca* 390 (CH_3CN)	–	–	–	–	$k_T = 0.01 \times 10^8$ (with perinaphthenone in D_2O)	–		
33	*ca* 360 (CH_3CN)	–	–	–	–	$k_T = 0.3 \pm 0.1 \times 10^8$ (D_2O buffer, pD *ca* 7.2)	–		
						$k_T = 7.9 \pm 0.2 \times 10^8$ (alkaline D_2O)			
34	*ca* 390 (CH_3CN)	–	–	–	–	$k_T = 0.01 \times 10^8$ (CH_3CN) $k_T = 0.3 \pm 0.05 \times 10^8$ (with MB in D_2O)	–		

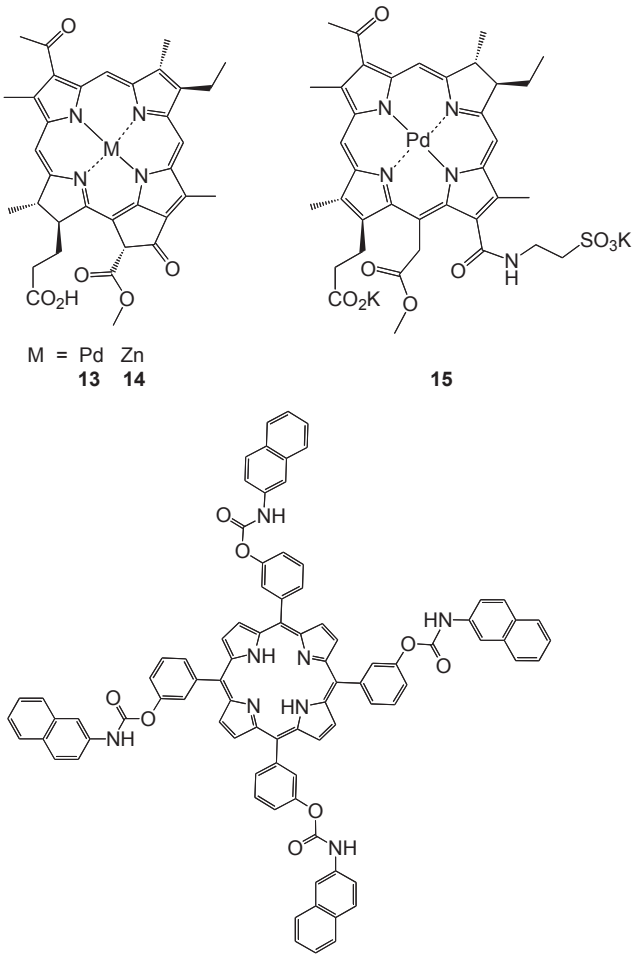

Scheme 4.

the triplet porphyrin and singlet oxygen quantum yields were found to be enhanced compared to the parent 5,10,15,20-tetra-(3-hydroxyphenyl)-porphyrin. Sensitizer **16** was also found to be photoactive against human carcinoma HT-29 cells.

SUPPORTS FOR OR ENCAPSULATION OF PHOTOSENSITIZERS

In addition to free sensitizers, researchers have been active in attaching or enclosing sensitizers by way of heterogeneous platforms and phases. Among other things, highly hydrophobic sensitizers can be solubilized *via* encapsulation in vesicles, liposomes or capsules for use in aqueous media.

Supports

The photolysis of protoporphyrin IX-supported silica nanoparticles sized 10, 25 or 60 nm led to the formation of singlet oxygen, which could diffuse out of the porous matrix (10). The short diffusion distance of singlet oxygen away from the nanoparticles (*ca* 20–150 nm) did not inhibit its ability to cause cell death in HCT 116 and HT-29 (colon cancer cells), MCF7 and MDA-MB-231 (breast cancer cells), A431 (epidermoid

cells) and LLBC37 (lymphoblastoid cells) and tumor destruction in mice.

The use of quantum dots as photosensitizers dates back only several years. CdTe quantum dots coated with thioglycolic acid sized *ca* 3.5 nm served as a unique photosensitizer capable of photodestruction of nasopharyngeal carcinoma cells (11). Low concentrations of singlet oxygen were found and Type-I photooxidations produced ROS that arose from the initial production of surface electrons.

Photooxidation mechanisms of DNA are difficult to study in biological systems. Making inroads to understanding the behavior of DNA damage, a photosensitizer [benzo[*a*]pyrene 7,8-diol 9,10-epoxide N^2-guanine (G_1^{Py})] was incorporated into the oligonucleotide 5′-d($CATG_1^{Py}CG_2TCCTAC$) to examine hole injection and migration. To appreciate the oxidative damage, an analysis was done of the Py-modified base, dG_1^{Py} and the guanine residue G_2 (12). The 355 nm irradiation of the pyrene sensitizer generated a $Py^{\bullet+}$ by a two-photon process, as well as hydrated electrons that were trapped by O_2 to form superoxide. An M + 16 nucleoside oxidation product was formed from the photosensitizing dG_1^{Py} moiety in which the cyclohexenyl ring opened with a carbonyl group at the rupture site. ^{18}O labeling studies showed that the oxygen atom originated from $H_2{}^{18}O$ and not from $^{18}O_2$.

Container systems and gels

Apoferritin was fragmented and found to self-reassemble and encapsulate methylene blue (13). The apoferritin container with methylene blue guests was cytotoxic against MCF-7 human breast adenocarcinoma cells with 633 nm light and activated singlet oxygen sensor green, a probe which has attracted attention recently due to its high fluorescence intensity in the presence of singlet oxygen. One study was concerned with topical photodynamic therapy applications and reducing sensitizer aggregation. Hydrophilic and lipophilic (Cremophor and Lutrol) gel formulations of tetra-*t*-butylphthalocyaninato zinc(II) (**17**), tetrakis(1,1-dimethyl-2-phthalimido)ethylphthalocyaninatozinc(II) (**18**), 2,3,9,10,16,17,23,24-octakis(decyloxy)phthalocyaninatozinc(II) (**19**) and 2,3,9,10,16,17,23,24-octakis[(*N*,*N*-dimethylamino)ethylsulfanyl]phthalocyaninatozinc(II) (**20**) were found to generate singlet molecular oxygen with Φ_Δ values ranging from 0.20 to 0.60 assessed with imidazole and the bleaching of *N,N*-diethyl-4-nitrosoaniline (Scheme 5) (14). When accumulated in the lipophilic gel, **17** and **18** bearing branched substituents were less aggregated than **19** and **20** bearing long-chain substituents.

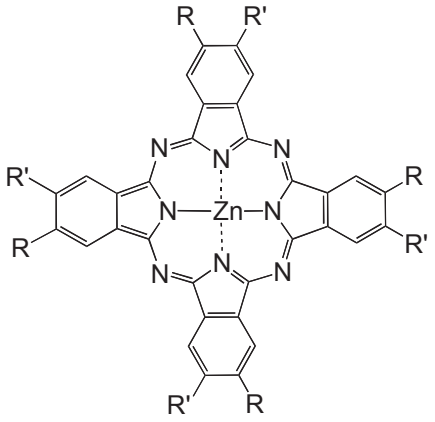

17: R = H; R' = $C(CH_3)_3$

18: R = H; R' =

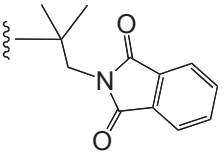

19: R = R' = $O(CH_2)_9CH_3$

20: R = R' = $S(CH_2)_2N(CH_3)_2$

Scheme 5.

PHOTOOXIDATION AND PHOTOPROTECTION REACTIONS

Photooxidation

6-Thioguanine (**21**) has a λ_{max} at 340 nm and was found to act as a Type-II photosensitizer, generating singlet oxygen upon UVA irradiation (15) (Scheme 6). The photooxidization products included guanine sulfenate, guanine sulfinate and guanine sulfonate, wherein the structures of the latter two were established unambiguously. Inclusion of *N*-acetylcysteine during the photooxidation not only protected **21** against oxidation, it produced an addition product, an amino-purinylthiopropanoic acid derivative (**22**). The photooxidations of tryptophan methyl ester (**23**) and tryptophan octyl ester (**24**) were carried out with perinaphthenone (PN) and RB in 1,2-dioleoyl-glycero-3-phosphatidylcholine (DOPC) vesicles, where **24** intercalated into the membrane to a greater extent due to higher hydrophobicity (16). Chemical and total quenching of $^1O_2$ were enhanced for **23** and **24** in water compared to DOPC liposomes. Tryptophan residues in proteins (**25**) reacted with $^1O_2$ to form *N*-formylkynurenine (NFK **26**) and hydroperoxide and hydrotryptophan products (17). Here, an anti-NFK antiserum was used in immunological assays, and its usefulness was reaffirmed for the specific detection of oxidized tryptophan residues in cells. One study dealt with the photodegradation of a pesticide, cyanophos (**27**). Cyanophos **27** was studied in aqueous solution with solar radiation or UV light in the 254–313 nm range, and in the presence and absence of hydroquinone (18). A photooxidation mechanism was implicated because of an increased degradation quantum yield in O_2-saturated than O_2-free solutions.

Photoprotection

Photoprotection mechanisms are also an area of current interest. Recent developments include porous wool fibers that were shown to have enhanced photostability against ''photoyellowing'' when TiO_2 nanoparticles were incorporated into the material as a UV-blocking agent (19). The wool was treated with citric acid as the cross-linking agent and 1-75 g L^{-1} TiO_2 was incorporated onto the wool surface. The inhibition of wool yellowing and oxygenation was attributed to UV blocking of aromatic absorbers, such as

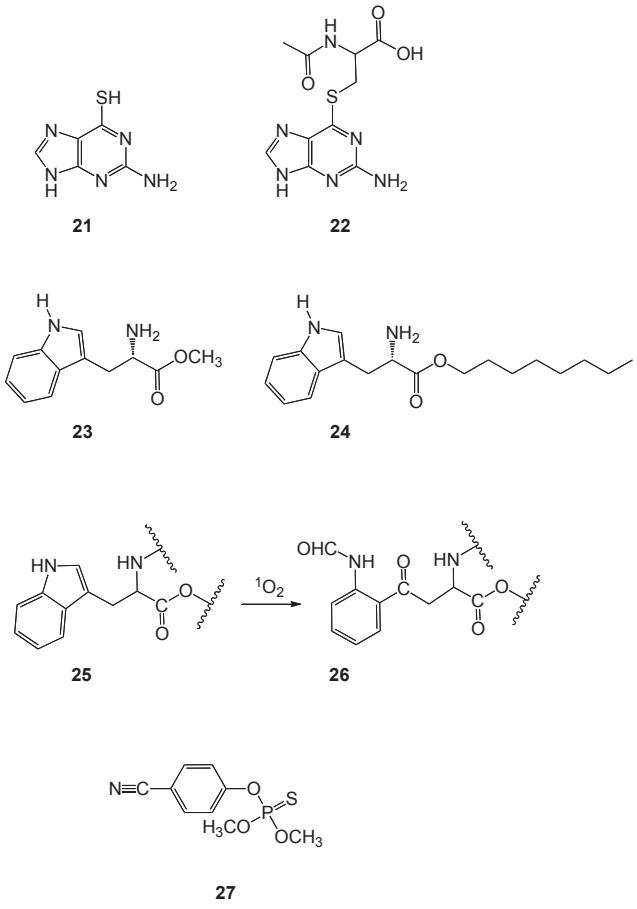

Scheme 6.

tryptophan. Besides TiO_2, flavones were another kind of photoprotective agents that were examined in two papers. (1) The photostability of the flavones quercetin (**28**), morin (**29**) and rutin (**30**) was examined with 450 nm light in riboflavin-sensitized photooxidations (Scheme 7) (20). Quercetin **28** was highly susceptible to photooxidation, whereas morin **29** and rutin **30** were less reactive. (2) Due to its photosensitivity, quercetin **28** was shown to stabilize UVA-absorber butyl methoxydibenzoylmethane and UVB-absorber octyl methoxycinnamate compounds (21). Photodegradation studies were followed in oil-in-water emulsions with a Xenon lamp. In this case, quercetin **28** was more effective than the other additives, octocrylene and vitamin E (butylated hydroxyanisole) and functioned to scavenge radicals *and* chelate metals, thereby slowing lipid peroxidation.

PHOTODYNAMIC ACTION

Major goals in photobiology are to understand how microbes are photoinactivated and tumors are destroyed. MB and RB sensitizers were used to photodynamically inactivate *Enterococcus faecalis* (22). The *E. faecalis* cells were examined as suspensions and biofilms. The biofilms were more resistant to photodynamic inactivation compared to the suspensions. Furthermore, it was advantageous to use MB in combination with verapamil hydrochloride (a specific microbial efflux pump inhibitor) to enhance the photodynamic inactivation of the *E. faecalis* biofilms. As would be expected, the presence of

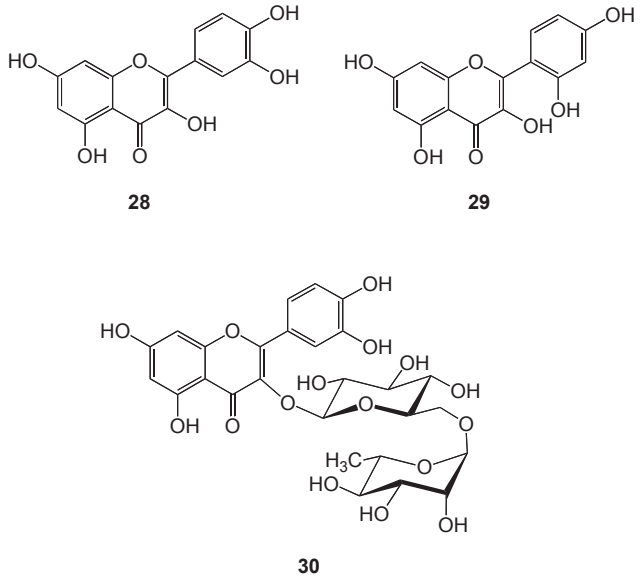

Scheme 7.

antioxidant pigments such as carotenoids or organic matter can reduce the efficiency of photodynamic inactivation of fungi (23).

Device development played a role in the construction of a hollow-core fiber-optic with an "internal" supply of light and flowing oxygen, and a porous photosensitizer end-capped configuration (24). The device delivered singlet oxygen through a maneuverable fiber tip, with handheld guidance. This led to complete *E. coli* inactivation when the sensitizing probe tip was immersed in 0.1 mL aqueous samples of $0.1–4.4 \times 10^7$ cells over 2 h.

A study of the natural product pyocyanin (1-hydroxy-5-methylphenazine, **31**) from the human pathogen bacterium *Pseudomonas aeruginosa*, and related phenazines (1-methoxy-5-methylphenazine methosulfate [**32**], 1-hydroxy-phenazine [**33**] and 5-methylphenazine methosulfate [**34**]) revealed how structural modifications played a role in the $^1O_2$ quenching (Scheme 8) (25). The total rate constants for $^1O_2$ quenching by pyocyanin **31** and phenazine **33** were rapid in D_2O buffer (pD *ca* 7.2) 4.8×10^8 and 6.8×10^8 M^{-1} s^{-1}, respectively. Phenazines **32** and **34** were sluggish in quenching $^1O_2$.

The use of metal-oxide and polymer-bound photosensitizers has been popular. Photocatalytic bactericidal activity toward *E. coli* with 30 nm diameter anatase TiO_2 nanocrystals was compared with TiO_2 powder (Degussa P-25) containing anatase and rutile phases in a ratio of about 3:1 with 400 nm light (26). The former was more active than the latter, which was attributed to less efficient charge recombination and higher ROS yields. Anatase Zr-doped TiO_2 nanocrystals (sized *ca* 25 nm) had a redshifted absorption spectrum (lower bandgap) compared to unmodified TiO_2 nanocrystals (27). In the presence of solar radiation, the photoinactivation of *P. aeruginosa* was enhanced with the Zr-doped TiO_2 by about two-fold because the doped samples were less apt to recombine charge. Anatase TiO_2 sol particles (spindle shaped, sized *ca* 50 nm) were synthesized and were found to inactivate H_9N_2 avian influenza virus (AIV) (28). 365 nm light was used with adjustments to the intensity, irradiation time and quantity of H_9N_2 AIV, where the inactivation of the AIV viruses reached quantitative levels, 100%. Due to aggregation in aqueous

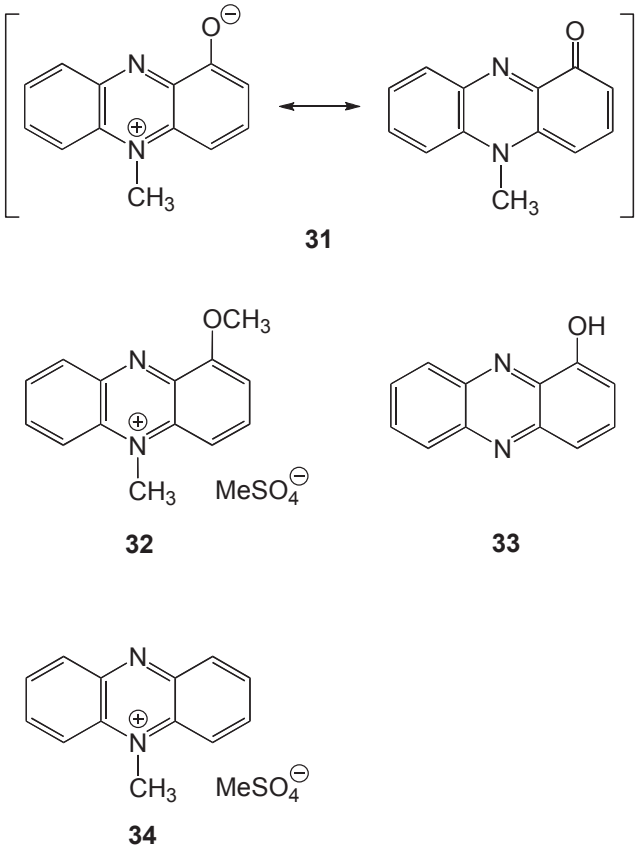

Scheme 8.

solution, water-dispersed TiO_2/PEG nanoparticles were also developed as a photosensitizer system (29). The nanoparticles were examined with monolayer and spheroid C6 rat glioma cells where the cell growth was reduced due to photoexcited TiO_2 itself and/or ROS. The TiO_2/PEG particles proved to have antitumor activity against C6 monolayer cells, but less so for the C6 spheroids, possibly due to reduced light penetration and low oxygen concentrations in the center of the spheroids.

With the aim of ultimately developing better food storage materials, anthraquinone was covalently incorporated into a polymer (**35**) (Scheme 9) (30). In the presence of oxygen and UVA radiation, exogenously produced singlet oxygen inactivated microbes that were inoculated onto the polymer surface. Out of the species inoculated (*E. coli*, *Bacillus cereus*, *Fusarium oxysporum* and *Saccharomyces cerevisiae*), *E. coli* was the least resistant and *B. cereus* the most resistant. The biocidal activity involved ROS contact at the microorganism/sensitizing polymer interfaces.

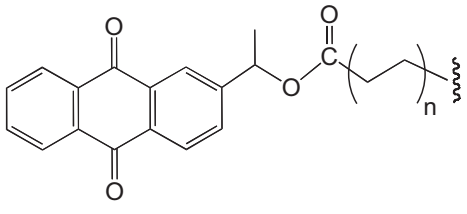

Scheme 9.

Photosensitizer dosimetry was assessed by photoacoustic signals from the photosensitizer in tissue in a study aimed at combating antibiotic-resistant bacteria. *In vivo* photoacoustic signals were resolved from MB or Photofrin that was injected into burned skin of rats for profiling of the sensitizer up to 3 mm in depth (31). Other themes in photodynamic action were also represented. One technique, chemiluminescent photodynamic antimicrobial therapy (CPAT) used light captured from a chemiluminescent luminol to excite MB or toluidine blue and was effective in killing *S. aureus* and inhibiting the growth of *E. coli* (32). In principle, CPAT can bypass the need of an external light source to activate the photosensitizer. Two papers analyzed hematoporphyrins: Hematoporphyrin monomethyl ether (HMME) was used to study PDT effects on choroidal neovascularization (CNV) in rats (33). The photodynamic treatment was performed for 20 min after HMME bolus injection and monitored by fluorescence microscopy where CNV occlusion was observed. Lastly, the photodynamic effects were examined on immature stages of diptera *Ceratitis capitata* flies with hematoporphyrin IX as the sensitizer (34). The lethal concentration (LC_{50}) of hematoporphyrin IX was found to be 0.173 mM based on a postembryonic development of the insect. Lipid peroxidation was particularly prevalent in the brain and gut of the larvae (34).

Acknowledgement—We acknowledge support from the National Institute of General Medical Sciences (NIH SC1GM093830).

AUTHOR BIOGRAPHIES

Bonnie Kruft

Bonnie Kruft was born near Chesapeake Bay in Maryland. She completed her B.S. degree in chemistry at The College of Charleston in Charleston, South Carolina in 2007. She is currently working toward her Ph.D. degree with Professor A. Greer at Brooklyn College of the City University of New York, engaged in computations and spectroscopy of self-replicating and helical molecules. She enjoys activities such as cooking, traveling and photography.

Alec Greer

Alec Greer obtained his Ph.D. degree from the University of Wyoming under Edward L. Clennan. He was a postdoctoral fellow at the University of California, Los Angeles with Christopher S. Foote and then moved to Brooklyn College of the City University of New York in 1999. His research interest is in physical organic chemistry, and is developing devices for use in water disinfection, and as a photochemical surgical knife or singlet oxygen scalpel.

REFERENCES

1. Otake, E., S. Sakuma, K. Torii, A. Maeda, H. Ohi, S. Yano and A. Morita (2010) Effect and mechanism of a new photodynamic therapy with glycoconjugated fullerene. *Photochem. Photobiol.* **86**, 1356–1363.
2. Cahan, R., N. Swissa, G. Gellerman and Y. Nitzan (2010) Photosensitizer–antibiotic conjugates: A novel class of antibacterial molecules. *Photochem. Photobiol.* **86**, 418–425.
3. Lai, S.-W., Y. Liu, D. Zhang, B. Wang, C.-N. Lok, C.-M. Che and M. Selke (2010) Efficient singlet oxygen generation by luminescent 2-(2′-thienyl)pyridyl cyclometalated platinum(II) complexes and their calixarene derivatives. *Photochem. Photobiol.* **86**, 1414–1420.
4. Theodossiou, T. A., D. Tsiourvas and J. S. Hothersall (2010) Hypericin hydroquinone: Potential as a red-far red photosensitizer? *Photochem. Photobiol.* **86**, 18–22.
5. Zhang, Y., L. Song, J. Xie, H. Qiu, Y. Gu and J. Zhao (2010) Novel surfactant-like hypocrellin derivatives to achieve simultaneous drug delivery in blood plasma and cell uptake. *Photochem. Photobiol.* **86**, 667–672.
6. Zimcik, P., M. Miletin, H. Radilova, V. Novakova, K. Kopecky, J. Svec and E. Rudolf (2010) Synthesis, properties and *in vitro* photodynamic activity of water-soluble azaphthalocyanines and azanaphthalocyanines. *Photochem. Photobiol.* **86**, 168–175.
7. Trivedi, E. R., B. J. Vesper, H. Weitman, B. Ehrenberg, A. G. Barrett, J. A. Radosevich and B. M. Hoffman (2010) Chiral *bis*-acetal porphyrazines as near-infrared optical agents for detection and treatment of cancer. *Photochem. Photobiol.* **86**, 410–417.
8. Dandler, J., B. Wilhelm and H. Scheer (2010) Photochemistry of bacteriochlorophylls in human blood plasma: 1. Pigment stability and light-induced modifications of lipoproteins. *Photochem. Photobiol.* **86**, 331–341.
9. Silva, P., S. M. Fonseca, C. T. Arranja, H. D. Burrows, A. M. Urbano and A. J. F. N. Sobral (2010) A new nonconjugated naphthalene derivative of *meso*-tetra-(3-hydroxy)-phenyl-porphyrin as a potential sensitizer for photodynamic therapy. *Photochem. Photobiol.* **86**, 1147–1153.
10. Simon, V., C. Devaux, A. Darmon, T. Donnet, E. Thiénot, M. Germain, J. Honnorat, A. Duval, A. Pottier, E. Borghi, L. Levy and J. Marill (2010) Pp IX silica nanoparticles demonstrate differential interactions with *in vitro* tumor cell lines and *in vivo* mouse models of human cancers. *Photochem. Photobiol.* **86**, 213–222.
11. Chen, J.-Y., Y.-M. Lee, D. Zhao, N.-K. Mak, R. N.-S. Wong, W.-H. Chan and N.-H. Cheung (2010) Quantum dot-mediated photoproduction of reactive oxygen species for cancer cell annihilation. *Photochem. Photobiol.* **86**, 431–437.
12. Yun, B. H., P. C. Dedon, N. E. Geacintov and V. Shafirovich (2010) One-electron oxidation of a pyrenyl photosensitizer covalently attached to DNA and competition between its further oxidation and DNA hole injection. *Photochem. Photobiol.* **86**, 563–570.
13. Yan, F., Y. Zhang, K. S. Kim, H.-K. Yuan and T. Vo-Dinh (2010) Cellular uptake and photodynamic activity of protein nanocages containing methylene blue photosensitizing drug. *Photochem. Photobiol.* **86**, 662–666.
14. Rodriguez, M. E., V. E. Diz, J. Awruch and L. E. Dicelio (2010) Photophysics of zinc (II) phthalocyanine polymer and gel formulation. *Photochem. Photobiol.* **86**, 513–519.
15. Ren, X., Y.-Z. Xu and P. Karran (2010) Photo-oxidation of 6-thioguanine by UVA: The formation of addition products with low molecular weight thiol compounds. *Photochem. Photobiol.* **86**, 1038–1045.
16. Posadaz, A., N. M. Correa, M. A. Biasutti and N. A. García (2010) A kinetic study of the photodynamic effect on tryptophan methyl ester and tryptophan octyl ester in DOPC vesicles. *Photochem. Photobiol.* **86**, 96–103.
17. Ehrenshaft, M., M. G. Bonini, L. Feng, C. F. Chignell and R. P. Mason (2010) Partial colocalization of oxidized, *N*-formylkynurenine-containing proteins in mitochondria and Golgi of keratinocytes. *Photochem. Photobiol.* **86**, 752–756.
18. Menager, M., J. F. Pilichowski and M. Sarakha (2010) Reaction pathways for the photodegradation of the organophosphorus cyanophos in aqueous solutions. *Photochem. Photobiol.* **86**, 247–254.
19. Montazer, M. and E. Pakdel (2010) Reducing photoyellowing of wool using nano TiO_2. *Photochem. Photobiol.* **86**, 255–260.
20. Montaña, M. P., W. A. Massad, S. Criado, A. Biasutti and N. A. García (2010) Stability of flavonoids in the presence of riboflavin-photogenerated reactive oxygen species: A kinetic and mechanistic study on quercetin, morin and rutin. *Photochem. Photobiol.* **86**, 827–834.
21. Scalia, S. and M. Mezzena (2010) Photostabilization effect of quercetin on the UV filter combination, butyl methoxydibenzoylmethane–octyl methoxycinnamate. *Photochem. Photobiol.* **86**, 273–278.
22. Kishen, A., M. Upadya, G. P. Tegos and M. R. Hamblin (2010) Efflux pump inhibitor potentiates antimicrobial photodynamic inactivation of *Enterococcus faecalis* biofilm. *Photochem. Photobiol.* **86**, 1343–1349.
23. Gonzales, F. P., S. H. Da Silva, D. W. Roberts and G. U. L. Braga (2010) Photodynamic inactivation of conidia of the fungi *Metarhizium anisopliae* and *Aspergillus nidulans* with methylene blue and toluidine blue. *Photochem. Photobiol.* **86**, 653–661.
24. Aebisher, D., M. Zamadar, A. Mahendran, G. Ghosh, C. McEntee and A. Greer (2010) Fiber-optic singlet oxygen $[^1O_2(^1\Delta_g)]$ generator device serving as a point selective sterilizer. *Photochem. Photobiol.* **86**, 890–894.
25. Reszka, K. J., P. J. Bilski and B. E. Britigan (2010) Quenching of singlet oxygen by pyocyanin and related phenazines. *Photochem. Photobiol.* **86**, 742–746.
26. Swetha, S., S. M. Santhosh and R. Geetha Balakrishna (2010) Synthesis and comparative study of nano-TiO_2 over degussa P-25 in disinfection of water. *Photochem. Photobiol.* **86**, 628–632.
27. Swetha, S., S. M. Santhosh and R. Geetha Balakrishna (2010) Enhanced bactericidal activity of modified titania in sunlight against *Pseudomonas aeruginosa*, a water-borne pathogen. *Photochem. Photobiol.* **86**, 1127–1134.

28. Cui, H., J. Jiang, W. Gu, C. Sun, D. Wu, T. Yang and G. Yang (2010) Photocatalytic inactivation efficiency of anatase nano-TiO_2 sol on the H_9N_2 avian influenza virus. *Photochem. Photobiol.* **86**, 1135–1139.
29. Yamaguchi, S., H. Kobayashi, T. Narita, K. Kanehira, S. Sonezaki, Y. Kubota, S. Terasaka and Y. Iwasaki (2010) Novel photodynamic therapy using water-dispersed TiO_2–polyethylene glycol compound: Evaluation of antitumor effect on glioma cells and spheroids *in vitro*. *Photochem. Photobiol.* **86**, 964–971.
30. Zerdin, K. and A. D. Scully (2010) Inactivation of food-borne spoilage and pathogenic micro-organisms on the surface of a photoactive polymer. *Photochem. Photobiol.* **86**, 1109–1117.
31. Hirao, A., S. Sato, D. Saitoh, N. Shinomiya, H. Ashida and M. Obara (2010) *In vivo* photoacoustic monitoring of photosensitizer distribution in burned skin for antibacterial photodynamic therapy. *Photochem. Photobiol.* **86**, 426–430.
32. Nakonechny, F., M. A. Firer, Y. Nitzan and M. Nisnevitch (2010) Intracellular antimicrobial photodynamic therapy: A novel technique for efficient eradication of pathogenic bacteria. *Photochem. Photobiol.* **86**, 1350–1355.
33. Fan, S., H. Qiu, H. Huang, Y. Gu and J. Zeng (2010) Effects of photodynamic therapy using hematoporphyrin monomethyl ether on experimental choroidal neovascularization. *Photochem. Photobiol.* **86**, 972–980.
34. Pujol-Lereis, L. M., A. Massaldi, A. Rabossi and L. A. Quesada-Allué (2010) Photosensitizing effect of hematoporphyrin IX on immature stages of *Ceratitis capitata* (Diptera: Tephritidae). *Photochem. Photobiol.* **86**, 639–644.